Trade-offs in a high CO_2 habitat on a subsea volcano: condition and reproductive features of a bathymodioline mussel

Giulia S. Rossi[1,3,*], Verena Tunnicliffe[1,2]

[1]Department of Biology, University of Victoria, Victoria, BC V8W 2Y2, Canada
[2]School of Earth & Ocean Sciences, University of Victoria, Victoria, BC V8W 2Y2, Canada
[3]*Present address:* Department of Integrative Biology, University of Guelph, Guelph, ON N1G 2W1, Canada

ABSTRACT: Northwest Eifuku submarine volcano (Mariana Volcanic Arc) emits very high concentrations of CO_2 at a vent where the mussel *Bathymodiolus septemdierum* experiences pH as low as 5.2. We examined how this natural setting of high pCO_2 influences shell, body, and reproductive condition. Calcification is highly compromised: at a given shell volume, shells from NW Eifuku weigh about half those from reference sites in the south Pacific, and dissolution of the inner shell is evident. However, the condition indices of some NW Eifuku mussels were equal to or higher than those from Lau back-arc basin and the New Hebrides Island Arc. NW Eifuku mussels in pH 5.2 fluids had the highest symbiont abundances in gill bacteriocytes, probably due to greater dissolved sulphide access. Excess energy demands imposed by high pCO_2 conditions appears moderated by adequate food availability through symbiont chemosynthesis. In the sample with the lowest body condition, gametogenesis was lagging, although all mussels in high pCO_2 had developing gonads and the complete gametogenic cycle was present in our samples. Gamete development is synchronous between sexes and is possibly periodic. While mussels are functionally dioecious, protogynous hermaphroditism can occur—a first record for the genus—which may be an adaptation to resource availability. *B. septemdierum* likely makes energy allocation trade-offs among calcification, body mass maintenance, reproduction and other processes to maximize fitness. We suggest that flexibility to divert energy from shell formation, combined with good food supply, can mitigate the manifestation of high CO_2 stress on *B. septemdierum*.

KEY WORDS: High pCO_2 · Hydrothermal vent · Calcification · Condition · Gametogenesis · Protogyny · Acidification

INTRODUCTION

Uptake of anthropogenic carbon dioxide is causing ocean acidification and a reduction in the ocean's buffering capacity; surface pH may decline by as much as 0.4 units by the year 2100 (Gattuso et al. 2015). Global outcomes for marine ecosystem services, including food production, are designated at high risk (IPCC 2014). Studies of acidification effects on organisms in laboratory and mesocosm conditions report a wide range of responses related to calcification, de-

velopment, behaviour and physiology (Ries et al. 2009, Kroeker et al. 2010, Branch et al. 2013). Consequences for calcifying organisms—mostly negative—are particularly notable, and compromised calcium carbonate structures have been reported from coral reefs (e.g. Silverman et al. 2014), aquaculture (Barton et al. 2012) and plankton (Bednarsek et al. 2014). An additional consequence is the accumulation of excess CO_2 in animal bodies. Hypercapnia is problematic in organisms that rely on favourable tissue-to-environment gradients for CO_2 excretion (Michaelidis et al.

2005, Gazeau et al. 2013). pCO_2 increases in the intra- and extra-cellular compartments of the body until a new CO_2 gradient can support CO_2 excretion (Seibel & Walsh 2003). However, a concomitant increase in $[H^+]$ can cause acidosis (Pörtner et al. 2004, Wicks & Roberts 2012) with consequences including metabolic depression, diminished protein synthesis and ammonia excretion, leading to lower overall fitness (see review by Gazeau et al. 2013). Acid–base regulation involves transmembrane transport of protons (Seibel & Walsh 2003, Pörtner et al. 2004), thus energy required to maintain homeostasis in response to acidification stress (Pan et al. 2015) is reallocated away from other processes such as skeletal deposition (Pörtner 2008).

Marine molluscs show a wide range of responses to acidification (both positive and negative) including calcification and immune responses, or even death (Gazeau et al. 2013). Effects on the mollusc shell reflect many factors including mineralogy and the ability to regulate pH at the calcification site (Ries et al. 2009). The life stage showing the most deleterious response is the mollusc larva (Barton et al. 2012, Gazeau et al. 2013), but studies on gametogenesis or reproduction are rare. In an extreme setting of high pCO_2 and low pH (to 5.4; Ω_{arag} ~ 0.01), bathymodioline mussel calcification and growth rates were half those measured in pH above 7.8 (Ω_{arag} > 1.7) (Tunnicliffe et al. 2009). The extent and density of mussels on the hydrothermally active summit of NW Eifuku volcano in the Mariana Arc (Embley et al. 2007) warrant a second look at how the acidic conditions may affect other aspects of condition and fitness. Uthicke et al. (2016) suggest field studies are important complements to manipulations to support predictions with a larger understanding of the ecological setting in which response to acidification is manifest.

Mytilid mussels of the genus *Bathymodiolus* occur at many hydrothermal vent and cold seep sites around the world, where dense beds provide habitat for many other species (Turnipseed et al. 2003). Nutrition is provided mainly by intracellular bacterial symbionts in the gills, but particulate feeding supplements this energy source in many species (Fisher et al. 1987, Page et al. 1991, Dubilier et al. 1998). Several species were described in the genus from the western Pacific, but here we adopt the molecular results of Breusing et al. (2015), who classified *B. brevior, B. elongatus* and *B. marisindicus as B. septemdierum* Hashimoto & Okutani. The resulting biogeographic spread from the Tongan Arc to the Izu-Bonin Arc to the Central Indian Ridge is the widest range reported for a vent species. Gametogenesis in species with supplemented particulate nutri-

tion appears to be seasonal, suggesting that phytodetritus can be a cue for spawning (Dixon et al. 2006, Tyler et al. 2007).

Condition indices that assess tissue weight to shell volume are effective tools to assess the physiological state of bivalves (Crosby & Gale 1990). Metabolic adjustments to support basal maintenance costs can deplete the carbohydrate and lipid reserves (Sokolova et al. 2012) in stressful conditions, including high pCO_2 (Lannig et al. 2010). In *Bathymodiolus*, good condition is related to optimal supply of reduced compounds that support endosymbiont chemosynthesis (Fisher et al. 1988, Nix et al. 1995, Bergquist et al. 2004). Given the high spatial and temporal variability in venting conditions across and within sites (e.g. Bates et al. 2013), mussels are likely to show a large range in condition. When stressors challenge an animal, energy allocation to maintenance generally takes precedence over growth and reproduction (Calow 1983, Sokolova et al. 2012). However, such trade-offs may reduce the ability to respond to additional stressors (Hochachka & Somero 2002, Pan et al. 2015), ultimately leading to reduced fitness.

NW Eifuku volcano in the Mariana Volcanic Arc emits the highest recorded concentrations of CO_2 for seafloor vents (Lupton et al. 2006). We examined whether this high pCO_2 habitat has serious consequences for tissue condition in the mussels that reflect a trade-off in resource allocation. Our objectives included (1) a test of the hypothesis that exposure to sustained high pCO_2 will result in poor body condition, (2) an assessment of gill and bacteriocyte characteristics, (3) a determination of whether gametogenesis and gonadal condition are compromised, and (4) a record of reproductive aspects of an important foundation species that inhabits hydrothermal vents throughout the west Pacific and Indian Oceans.

MATERIALS AND METHODS

Field sampling

Bathymodiolus septemdierum specimens were collected between April 2004 and April 2016 at 3 vent fields in the western Pacific (Table 1). Northwest Eifuku is a submarine volcano on the Mariana Volcanic Arc, northwest Pacific. At 1610 m depth, 80 m south of the summit, Champagne Vent discharges gas-rich fluids with H_2S and liquid CO_2 (Lupton et al. 2006). The resultant hydrothermal plume circulates around the summit, sustaining a mussel bed ~10 000 m^2 in

Table 1. *Bathymodiolus septemdierum* collection site and sample characteristics; NWE: Northwest Eifuku

Site	Region	Expedition	Site coordinates (°N, °E)	Date	Depth (m)	No. mussels collected	Preservation method
NWE One	NWE, Mariana Volcanic Arc	RR1413	21.4875, 144.0414	13-Dec-14	1605	38[a]	Formalin/ frozen
NWE Two	NWE, Mariana Volcanic Arc	RR1413	21.4876, 144.0413	13-Dec-14	1606	45[a]	Formalin/ frozen
NWE Three	NWE, Mariana Volcanic Arc	RR1413	21.4875, 144.0418	06-Dec-14	1561	33[a]	Formalin/ frozen
NWE Four	NWE, Mariana Volcanic Arc	SRoF'04	21.4878, 144.0417	10-Apr-04	1576	30	Formalin
Nifonea	Vate Trough, New Hebrides Island Arc	SO229	−18.133, 169.517	13-Jul-13	1873	23	Ethanol
ABE	East Lau Spreading Centre, Lau Basin	FK160407	−20.7626, 176.1918	25-Apr-16	2130	15	Formalin

[a]Gill snips of 2 mussels were fixed in 2.5% glutaraldehyde and 0.1 M PBS for transmission electron microscopy (TEM) analysis

extent where densities reach 250 ind. m^{-2} (Tunnicliffe et al. 2009). Several visits with remotely operated vehicles over a decade confirmed relatively stable hydrothermal flux. In April 2004, we collected mussels from one site on NW Eifuku (NWE Four) where pH and $[H_2S]$ were determined from water samples collected with a multi-chambered manifold (Tunnicliffe et al. 2009). From each mussel, one valve was removed, and the remaining valve and body were fixed in 7% buffered formalin.

In December 2014, we retrieved mussels from 3 more sites: NWE One, NWE Two and NWE Three. At this time, pH measurements were taken *in situ* using an AMT Deep Water pH sensor. At all NW Eifuku collection sites, careful probing among the mussels detected consistent water conditions in the immediate environment of the animals. Shipboard, mussels were opened and weighed; an anterior gill snip from mussels at each site was fixed with 2.5% glutaraldehyde in 0.1 M phosphate-buffered saline (PBS) for transmission electron microscopy (TEM) analysis. One valve was removed from each mussel, and the remaining valve and body was either fixed in 7% buffered formalin or frozen at −80°C. Mussels were returned to the ship within a few hours of collection, except for retrieval from NWE Three, when weather conditions forced the vehicle and collected mussels to remain at ~1000 m depth for 2 d. NW Eifuku collection sites were separated by a maximum of ~100 m. As time and weather constraints limited sampling, in this study we refer to $[H_2S]$ measurements taken in similar pH and temperature conditions in this mussel bed from a previous study (Tunnicliffe et al. 2009).

We compared the mussels to 'reference' sites where evidence for high pCO_2 is lacking and mussels have thicker shells. The Nifonea field in the New Hebrides Island Arc near Vanuatu sits on a large axial volcano in the Vate Trough. Hydrothermal activity in the northeast sector of the summit caldera supports tubeworms, mussels and other vent fauna (Anderson et al. 2016). Our collection site is characterized by diffuse hydrothermal fluids emanating from pillow lavas and fractures, where mussels are dense around focused venting, but are patchy in peripheral cracks between pillow lavas. In July 2013, mussels were retrieved from a diffuse vent, but no water measurements were made. Mussels were preserved in 95% ethanol.

Also in the southwest Pacific, the Lau back-arc basin hosts several vent fields along the Eastern Lau Spreading Centre (Flores et al. 2012). In April 2016, a vehicle retrieved mussels from the ABE site characterized by Podowski et al. (2009, 2010). Although we have no water information from directly among the mussels, temperature was measured over a small mass of snails, *Ifremeria nautilei*, that was surrounded by the collected mussels. Both valves were removed, and the mussel body was fixed and stored in 7% buffered formalin.

Condition

The relationship between shell weight and volume (W:V) was compared across collection sites using one undamaged valve from each mussel. Any attached epifauna was removed before weighing. Shell volume was determined as double the amount of water one

valve could hold. Shell length was measured to the nearest mm. Water content (as a percentage of tissue mass) of NWE One, NWE Two and NWE Three mussels was determined from wet body weights measured prior to preservation in 7% formalin shipboard. Body and gill condition indices were compared among sites following methods developed by Higgins (1938). Gills were dissected from the body, and the ash-free dry weight (AFDW) of each component was determined after drying at 60°C and burning at 550°C in a muffle furnace. Prior to drying, symbiotic scale worms were removed from Nifonea mussels, but no such polynoids inhabited NW Eifuku or ABE mussels. There is no difference in body weight change between preservation methods (Mills et al. 1982). Condition indices (CI) were determined using the following equations:

$$BCI = (\text{body AFDW / shell volume}) \quad (1)$$

$$GCI = (\text{gill AFDW / shell volume}) \quad (2)$$

$$CI = (\text{body AFDW + gill AFDW}) / \text{shell volume} \quad (3)$$

where BCI and GCI are body and gill condition index, respectively

Due to similarities between female and male condition indices, mussels of both sexes were combined for analysis at each site.

TEM and histology

Two mussels between 100 and 130 mm in length from NWE One, NWE Two and NWE Three were selected for TEM analysis. The fixed gill snips were rinsed in 0.1 M PBS, post-fixed in 1% osmium tetroxide, dehydrated in an ethanol series and propylene oxide, and embedded in EMbed 812 resin. Ultrathin cross-sections of the mid-filament region of the gill tissue were stained with uranyl acetate and lead citrate. The sections were examined using a JEOL JEM-2100F transmission electron microscope. ImageJ software was then used to measure bacterial layer thickness, symbiont diameters and symbiont abundance in each photographed section. Symbiont abundance was calculated by randomly selecting one 25 μm^2 area from the apical (symbiont-bearing) region of 3 bacteriocytes in each mussel, and determining the proportion of area occupied by symbionts in the selected region.

Sections of 5 mm thickness from the posterior gonad, anterior gonad and mantle/digestive gland were dissected from formalin-fixed mussels (Table 2). Tissues were dehydrated in a graded ethyl alcohol series and embedded in a JB-4 plastic resin solution. Transverse sections of 4 μm thickness were stained with hematoxylin and eosin. Gametogenesis was scored according to the staging scheme of Dixon et al. (2006) for *Bathymodiolus azoricus* with modifications specific to *Bathymodiolus septemdierum*. The gonadal index for each site was calculated according to Seed (1969): Gonadal index = Σ(no. of ind. in stage $x \times x$) / no. of all staged ind., where x is the numerical value of the stage.

Circular equivalent diameters were determined for 40 oocytes sectioned through the nucleus in each transverse section (totalling 120 oocytes ind.$^{-1}$) to construct oocyte size–frequency distributions. We calculated oocyte area from measures of longest and shortest axes of each oocyte, then derived circular equivalent diameter. Histology for ethanol-preserved mussels from Nifonea was not possible since ethanol did not adequately preserve cell structures.

Statistical analysis

Shell W:V ratio, CI, GCI, oocyte size and symbiont abundance data from each collection were assessed for normality using the Shapiro-Wilk test. When assumptions for parametric tests were not satisfied, a non-parametric Kruskal-Wallis test was used to compare across sites, and when assumptions were satisfied, an analysis of variance (ANOVA) was used to compare across sites. Linear regressions were performed to test the significance between % water content and CI, and GCI and BCI. Significance was designated at $\alpha < 0.05$ for all data analyzed. The number of mussels used in each analysis is summarized in Table 2.

Table 2. Number of *Bathymodiolus septemdierum* specimens from each site used in each analysis. TEM: transmission electron microscopy; NWE: Northwest Eifuku

Site	Shell measured	Body and gill condition	Gill TEM	Sex determination	Histology ♂/♀	Oocyte diameter
NWE One	38	12	2	25	6/6	6
NWE Two	45	12	2	30	7/5	5
NWE Three	33	12	2	24	6/6	6
NWE Four	27	15	0	30	6/6	6
Nifonea	27	15	0	27	0/0	0
ABE	14	9	0	15	6/2	2

RESULTS

Site characteristics

The pH values across NW Eifuku collection sites ranged from 5.22 to 7.30, and temperature was low, averaging 2.6 ± 0.1°C; pH was lower just above the mussels, increasing downward to the value presented in Table 3. At the lowest pH, we probed several points in the *Bathymodiolus septemdierum* clump (all values <5.3), then moved the probe about 50 cm laterally to a sedimented surface with no mussels; here, pH was 4.8. An H_2S concentration of 101 µmol l^{-1} was measured at NWE Four. In 2006, mussels were collected within 10s of m of the 2014 sites where [H_2S] ranged from 155 µmol l^{-1} (pH 5.36) to 1 µmol l^{-1} (pH 7.29) (Tunnicliffe et al. 2009), indicating that as pH decreases, dissolved sulphide increases on this volcano. Low pH was manifest in the large numbers of valves from dead mussels that consisted of decaying periostracum with no calcium carbonate remaining. Only on the farthest margins of the mussel bed did shells retain some white inner surface.

No CO_2 bubbles were present at the Nifonea site. Here, dead mussel shells with exposed inner aragonite surfaces were abundant in the beds, as were other animals with calcium carbonate skeletons such as barnacles, serpulids and crabs; such taxa are absent from NW Eifuku. At the ABE site, CO_2 in end member fluids was comparatively low, around 3 mmol kg^{-1} fluid (Mottl et al. 2011); in that study, pH was >7.0 around mussels in temperatures of 11 to 14°C. For our ABE sample, temperature over the adjacent *Ifremeria* snails was 15.3°C (R. Beinart pers. comm.) although it was likely lower among the mussels.

Table 3. Fluid characteristics at *Bathymodiolus septemdierum* collection sites in western Pacific Ocean. n/a: not available; 'co-located': sulphide concentration measured during sampling; 'inferred': sulphide concentration among mussels at a nearby location of similar pH (Tunnicliffe et al. 2009)

Site	Temp (°C)	pH	[H_2S] (µmol l^{-1}) (co-located)	[H_2S] (µmol l^{-1}) (inferred)
NWE One	2.7	5.22	n/a	155
NWE Two	2.7	5.78	n/a	n/a
NWE Three	2.6	6.98–7.30	n/a	~1
NWE Four	2.5	5.88	101	n/a
Nifonea	n/a	n/a	n/a	n/a
ABE	15.3[a]	n/a	n/a	n/a

[a]Water measured above snails within 50 cm

Shell condition

Mussel shells from NW Eifuku weighed significantly less than comparison sites (Kruskal Wallis: $\chi^2 = 97.75$, p < 0.001). At a given shell volume, weights were about half those from Lau Basin and Nifonea (Fig. 1A). The shell W:V relationship of NW Eifuku shells was relatively constant despite pH variability across collection sites, with the least calcified shells at NWE Two. The relationship between total body AFDW and shell weight was variable across all collection sites (Fig. 1B). NWE One mussels showed the highest body to shell weight ratio of all sites; these shells also displayed the greatest increase in volume with length (data not shown), indicating they can accommodate relatively more body mass at larger
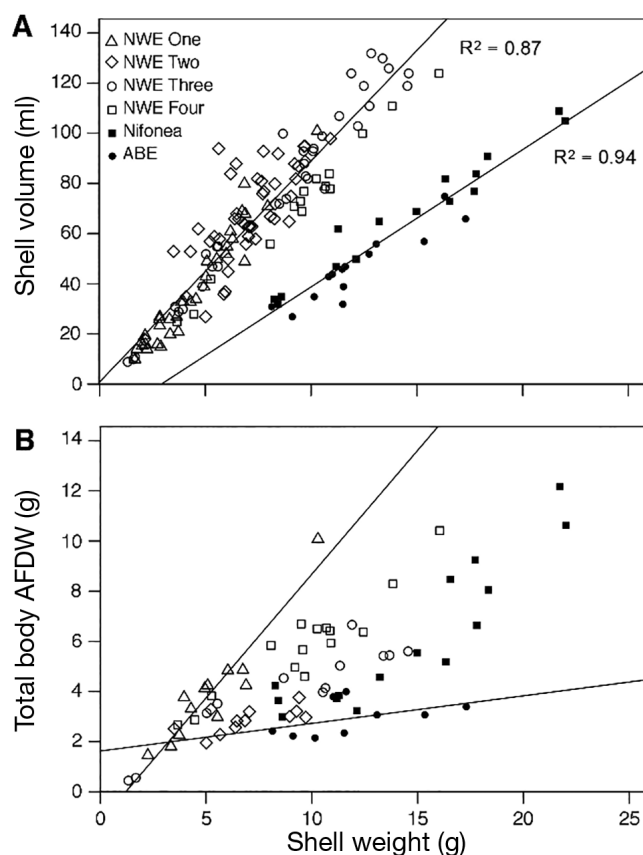

Fig. 1. *Bathymodiolus septemdierum* specimens collected from NW Eifuku and 2 'reference' sites. Open symbols: low pH sites; closed symbols: sites with greater calcification and likely higher pH. (A) Relationship between shell (1 valve) volume and weight illustrating markedly lower calcification at a given size on NW Eifuku, and (B) relationship between total body ash-free dry weight (AFDW) and shell weight showing highest body weight to shell weight ratio in NW One and lowest in the ABE specimens. Lines: regressions of these extreme relationships

sizes. NWE Two and ABE mussels exhibited the lowest body to shell weight ratio. We also noted signs of post-deposition dissolution on the inner surface of the NWE shells presenting as dull and rough. Prior scanning electron microscopy (SEM) images showed etched crystals (Tunnicliffe et al. 2009).

Condition indices

There was significant variation in body plus gill CIs across sites, including among mussels at neighbouring sites on NW Eifuku (Kruskal Wallis: $\chi^2 = 48.04$, p < 0.001; Fig. 2). The CI of mussels collected from NWE One and NWE Four were significantly higher than those of NWE Two and NWE Three (Wilcoxon rank-sum test, p < 0.05). Despite low pH conditions at NW Eifuku, the CI of NWE One and NWE Four mussels did not significantly differ from Nifonea, neither did NWE Four mussels differ from ABE (Wilcoxon rank-sum test, p > 0.05 for both). The degree to which reproductive tissues (gonad and mantle) contribute to CI likely varies based on gonadal development and fecundity, but it was not possible to excise these integrated tissues to examine contribution. The mean (±SD) % water content of NWE One, NWE Two and NWE Three mussels was 89.7 ± 2.1, 92.7 ± 1.7 and 91.4 ± 1.3 % respectively, with a significant negative relationship between CI and % water content (regres-

sion: $F = 33.07$, n = 36, p < 0.001; see Fig. S1 in the Supplement at www.int-res.com/articles/suppl/m574 p049_supp.pdf). Over 55 % of Nifonea mussels hosted scale worms *Branchipolynoë pettiboneae* within the mantle cavity — some with as many as 4 worms.

The relative contribution of *B. septemdierum* gills to total body mass for the 5 samples ranged from 17 to 26 %, with highest gill contribution in NWE Two mussels; a higher GCI coincided with a higher BCI (regression: $F = 73.07$, n = 75, p < 0.001; Fig. 3). The GCI across collection sites varied (Kruskal-Wallis: $\chi^2 = 47.93$, p < 0.001): mussels from NWE One, NWE Four and Nifonea had a significantly higher GCI than those of NWE Two, NWE Three and ABE (Wilcoxon rank-sum test, p < 0.05). We also examined body AFDW with respect to shell length (Fig. 4). Dry

Fig. 3. Relationship between mussel *Bathymodiolus septemdierum* gill condition index (GCI) and body condition index (excluding gills) is significant (Pearson correlation p < 0.05); however, the NW Eifuku sites tend to fall below the line
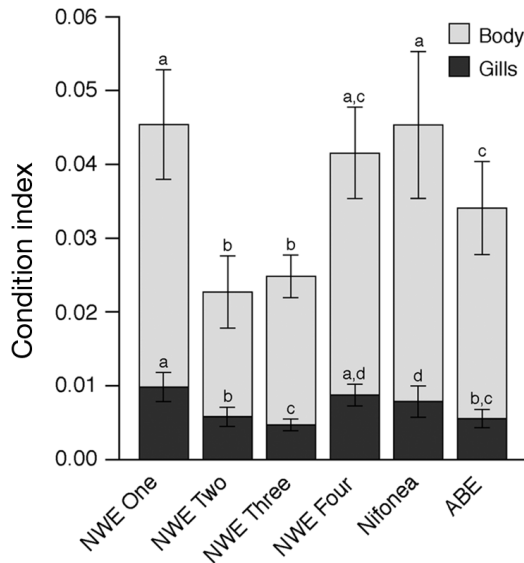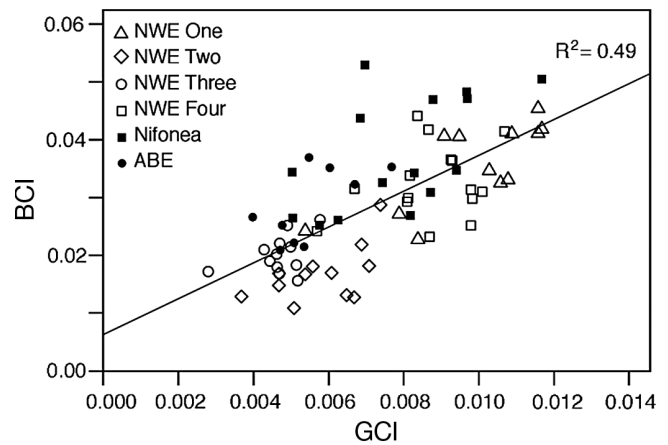

Fig. 2. Proportion of the condition index (CI) attributed to gill tissue and body tissue of mussels *Bathymodiolus septemdierum* from all sites. Letters denote statistically significant differences (p < 0.05) in gill condition index (GCI) and total body condition index (BCI) across sites. Error bars: SD for GCI and BCI (excluding gills). NW Eifuku has samples with both relatively high and low condition
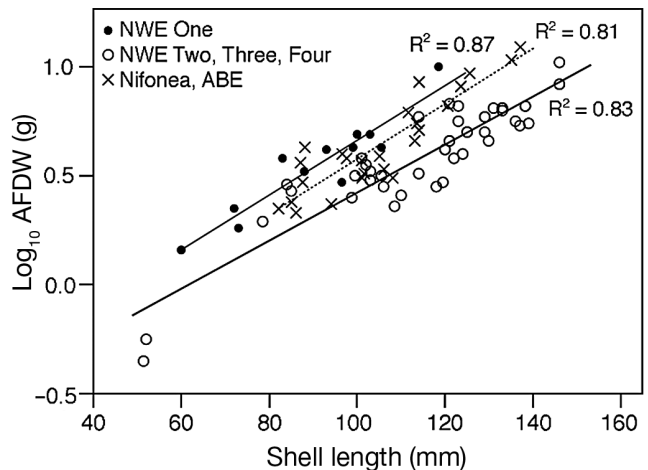

Fig. 4. Ash-free dry weight (AFDW) versus length shows that NWE One is similar to the reference sites; the remaining NW Eifuku sites tend to have more slender shells with less body mass

weight at a given shell length in NWE One mussels was more similar to our reference sites, while the remaining NWE mussels showed lower dry weight at length.

Gill structure

Overall structure of the gills in *B. septemdierum* was similar to that described in other species of the genus (Fisher et al. 1987, Fiala-Médioni et al. 2002). The lateral zone of the gill filament contained symbiont-bearing bacteriocytes and intercalary cells with a microvilli-covered apical surface. The cytoplasm near the apical region of the bacteriocyte was dominated by vacuoles containing symbiotic bacteria. NWE One mussels had as many as 12 bacteria vacuole^{-1}, which were often interconnected (Fig. 5A). Mussels from NWE Two and NWE Three typically had 1 or 2 bacteria vacuole^{-1}, though as many as 5 can occur (Fig. 5B). The thickness of this bacterial layer varied across collection sites. NWE One mussels had the thickest bacterial layer reported in this species (~25 µm; Fig. 5A), while that of NWE Two and NWE Three were thinner (~12 µm; Fig. 5B). Symbiont abundances differed significantly across sites (ANOVA: $F = 4.11$, p = 0.04); symbionts from NWE One were significantly more abundant than that of NWE Two (Tukey test, p < 0.05) (Table 4). More images are available in Rossi (2016). Gill symbionts were thiotrophic and the coccoid shape of the bacteria ranged from 0.25 to 0.75 µm in diameter. Bacteria had cytoplasmic and outer membranes typical of Gram-negative bacteria, and lacked intercytoplasmic membranes characteristic of methanotrophic bacteria.

Beneath the bacterial layer, the distal portion of bacteriocytes contained mucus granules, a well-defined nucleus surrounded by endoplasmic reticulum, mitochondria and lysosomes (Fig. 5A). Lysosomal degradation of bacteria was apparent in all mussels where membrane whorls were visible within secondary lysosomes. Intercalary cells (Fig. 5B) were
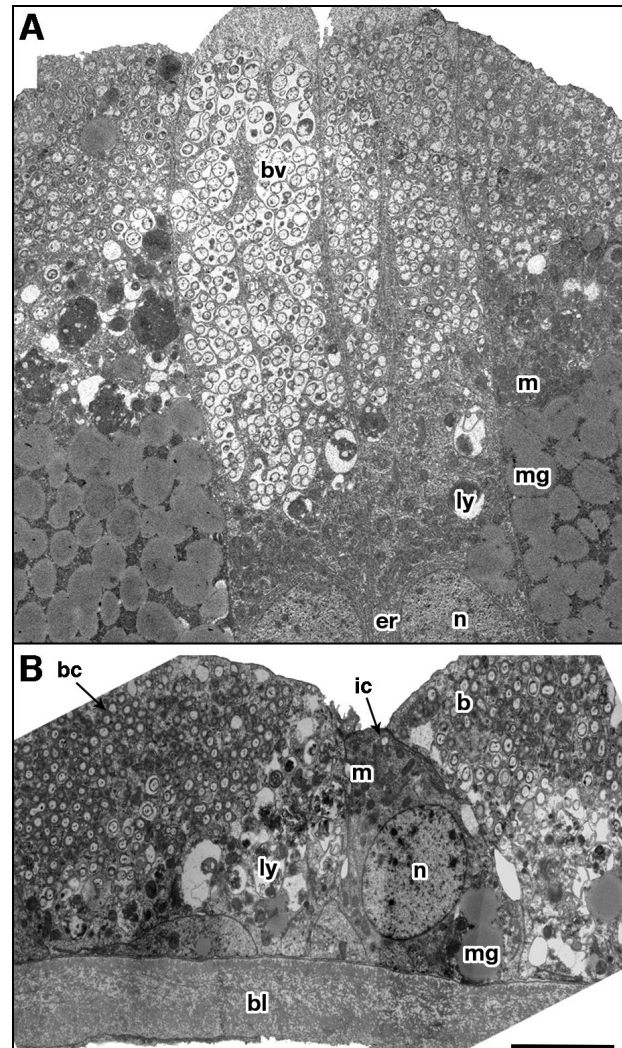

Fig. 5. Transmission electron microscopy (TEM) images of mussel *Bathymodiolus septemdierum* gills. (A) Cross-section through several bacteriocytes of NWE One mussel showing a broad bacterial layer and multiple bacteria within a vacuole, and (B) cross-section through NWE Three mussel gill where the bacteriocyte layer is narrow with fewer bacteria in a vacuole. bv: bacterial vacuole; m: mitochondria; mg: mucus granules; ly: lysosomes; er: endoplasmic reticulum; n: nucleus; bc: bacteriocyte; ic: intercalary cell; b: symbiotic bacteria; bl: basal lamina. Scale bar: 5 µm for both images

Table 4. Mean mussel shell length, sex, gametogenic features, and symbiont area of *Bathymodiolus septemdierum* from west Pacific collection sites. NWE: Northwest Eifuku; M:F: male to female ratio; n/a: not available. See Table 2 for sample sizes

Site	Mean (±SD) shell length (mm)	M:F ratio	Male gonadal index	Female gonadal index	Mean (±SD) oocyte diameter (µm)	Proportion (±SD) symbiont area
NWE One	87 ± 17	1.27	5.00	4.67	41 ± 6	0.36 ± 0.06
NWE Two	109 ± 12	0.30	3.86	3.60	33 ± 8	0.29 ± 0.01
NWE Three	112 ± 27	0.71	4.83	4.83	40 ± 6	0.29 ± 0.05
NWE Four	121 ± 25	0.25	2.83	2.50	33 ± 6	n/a
Nifonea	111 ± 16	0.93	n/a	n/a	n/a	n/a
ABE	92 ± 19	9.00	2.33	2.50	30 ± 10	n/a

small, and their ciliated apical surface was often concealed because they were fully enclosed by neighbouring bacteriocytes.

Size and sex ratio

Shell length distributions from all 5 sites were predominately left-skewed with a maximum length of 157 mm. The smallest average shell length occurred at NWE One and the largest at NWE Four. All individuals were sexually mature, with the smallest mussel being a 29 mm male, and the smallest female, 73 mm. Seventy-five percent of individuals <100 mm in length were male while 73 % of individuals >100 mm in length were female. Both males and females occurred among the largest individuals sampled. Male to female ratios varied among sites, and at ABE males greatly outnumbered females (Table 4). Evidence of sequential hermaphroditism was present only in ABE mussels, where sex change was from female to male. In 4 of 15 ABE mussels, residual oocytes remained in spawning canals and around the periphery of acini in functionally male mussels (Fig. 6). These protogynous mussels ranged from 81 to 102 mm in length. In all other mussels, only 1 type of gamete was present throughout the reproductive tissues.

Gametogenesis

Oogenesis and spermatogenesis stages are summarized in Table 5. In both sexes, gonad and mantle contain acini and gonadal ducts surrounded by interacinal tissue housing the adipogranular lipid storage cells that eventually convert to reproductive tissue. Acini numbers increase as gametogenesis proceeds uniformly throughout the gonad and mantle. Gonadal ducts often contain residual gametes. Most residual oocytes show signs of degradation including a grainy appearance, close proximity to haemocytes and disappearing nuclei; gamete degradation in males is less evident. In previously spawned individuals, residual oocytes may be present in deflated acini or gonadal ducts (Stage 1). Oogenesis initiates when the undifferentiated germ cells lining the acinus give rise, by mitotic division, to previtellogenic oocytes (Stage 2). During the subsequent stages (3 through 6; Table 5), oocytes enlarge and detach from the acinus wall as the extent of adipogranular tissue diminishes and spawning ensues. After spawning, haemocytes enzymatically degrade most of the residual oocytes (Stage 7).
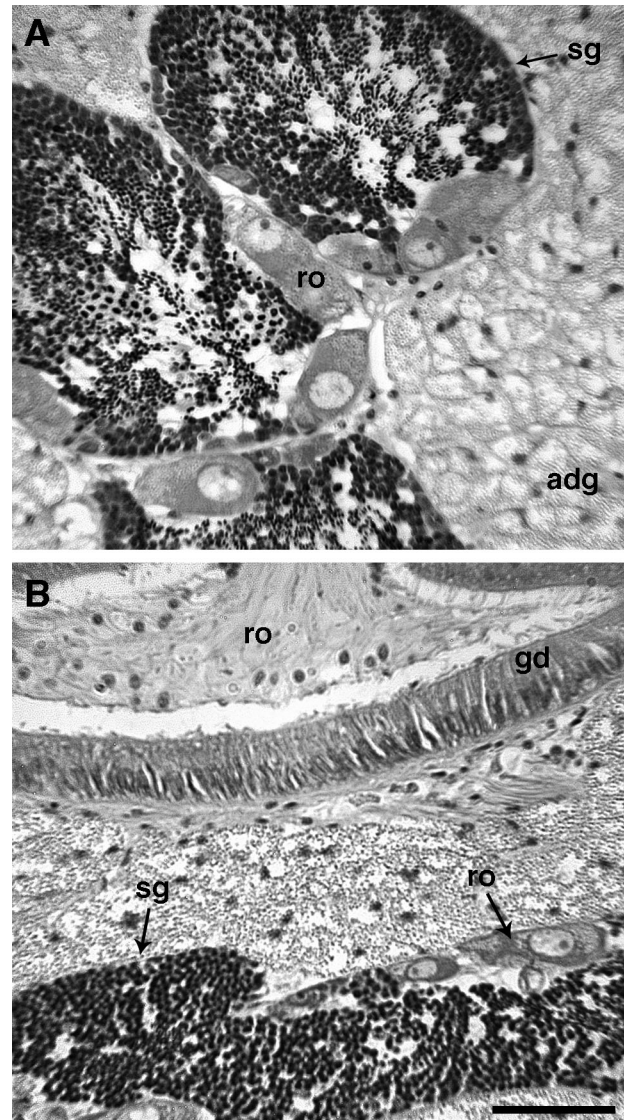

Fig. 6. Histological section of gonadal tissue in protogynous mussel *Bathymodiolus septemdierum* from ABE sample. (A) Functional male with residual oocytes along the periphery of the acinus, and (B) the same male with residual oocytes in the gonadal duct and in the acinus. sg: spermatogonia; ro: residual oocytes; adg: adipogranular cells; gd: gonadal duct. Scale bar: 50 μm

Spermatogenesis begins when spermatogonia and spermatocytes proliferate around the periphery of the acinus (Stage 2). Progression (Stages 3 thorough 5) then relates to degrees of proliferation of spermatids, differentiation into spermatozoa, and formation of spermatogonia (Table 5). During spawning, acini deflate and spermatozoa density is greatly reduced (Stage 6). After spawning, haemocytes degrade most of the residual spermatozoa (Stage 7).

Table 5. Stages of gametogenesis in *Bathymodiolus septemdierum*. Adapted from staging for *B. azoricus* (Dixon et al. 2006)

Stage	Oogenesis	Spermatogenesis
1a	Adipogranular cells only, sexually immature	Adipogranular cells only, sexually immature
1b	Residual oocytes may be present in sexually mature individuals within acini or gonadal ducts. Most tissue comprised of ADG cells	Residual spermatozoa may be present in sexually mature individuals within acini or gonadal ducts. Most tissue comprised of ADG cells
2	Initiation of gametogenesis: oogonial (previtellogenic) stage only. Residual oocytes may be present	Initiation of gametogenesis: proliferation of spermatogonia and spermatocytes around the periphery of the acinus. Residual spermatozoa may be present
3	Early gametogenesis: nothing beyond early vitellogenesis. Residual oocytes may be present	Early gametogenesis: spermatocytes begin to differentiate into spermatids and proliferate in lumen of acinus. Residual spermatozoa may be present
4	Late gametogenesis: late vitellogenic oocytes. Only basal region of the oocytes remains connected to acinus wall. Residual oocytes may be present	Late gametogenesis: spermatids fill the lumen and are connected by cytoplasmic material that forms swirls. Spermatogonia and spermatocytes only occupy periphery of acinus. Residual spermatozoa may be present
5	Gamete maturation: mature oocytes are released from acinus wall and fill acinus. The amount of adipogranular tissue is greatly reduced	Gamete maturation: spermatids differentiate into spermatozoa and gamete density increases. Amount of adipogranular tissue is greatly reduced
6	Spawning: gamete density is greatly reduced. Gonadal ducts visible in the intact mantle. Residual oocytes may be present	Spawning: gamete density is greatly reduced. Gonadal ducts visible in the intact mantle. Residual spermatozoa may be present
7	Post-spawning: massive haemocyte infiltration resulting in enzymatic degradation of residual gametes. Parts of the mantle now appear extremely thin, almost transparent in places	Post-spawning: massive haemocyte infiltration resulting in enzymatic degradation of residual. Parts of the mantle now appear extremely thin, almost transparent in places

Timing of gametogenesis

Timing of gametogenesis is reflected in gonadal indices and distribution of oocyte diameters summarized by size–frequency histograms (Figs. 7 & S2 in the Supplement). Approximately 40% of all measured oocytes from NWE Four and ABE samples were residual, and non-competent, from a prior spawning event—these large oocytes were excluded from analysis (Fig. 7). Non-residual April oocytes were significantly smaller than oocytes in December counterparts (Kruskal-Wallis: χ^2 = 1216.45, p < 0.01; Wilcoxon rank-sum test, p < 0.05). Mussels collected in December from NWE One and NWE Three had gonadal indices that correspond to Stages 4 or 5 (late gametogenesis/gamete maturation) and had the largest oocytes (Fig. 8). NWE Two mussels, also collected in December, lagged in development, with gonadal indices corresponding to Stages 3 or 4 (early to late gametogenesis); mean oocyte diameter was ~19% smaller than those at NWE One and Three. Mussels collected in April from both ABE and NWE Four were in the early stages of gametogenesis: gonadal indices correspond to Stages 2 or 3.

DISCUSSION

Habitat

On NW Eifuku, venting fluids have CO_2 concentrations as high as 2700 mmol kg^{-1} (Lupton et al. 2006), a value 3 orders of magnitude higher than ABE end member fluids at 6.0 mmol kg^{-1} (Mottl et al. 2011). To date, NW Eifuku has the highest pCO_2 measured at vents. The delivery of CO_2 as a liquid on NW Eifuku appears to affect its persistence in a visible sulphur-laden plume over the volcano summit. In neither this study nor that of Tunnicliffe et al. (2009) was fluid egress detected under the mussels, where temperature was ambient and pH was higher than directly above the mussels. Instead, vent fluid is delivered laterally over the mussel bed in a manner influenced by plume dynamics and distance from Champagne Vent. Consequently, there are no small-scale changes in local venting that mobile mussels could exploit to escape localized conditions that exceed tolerance limits. The only notable 'zonation' is diminishing mussel density at the edge of the large field.
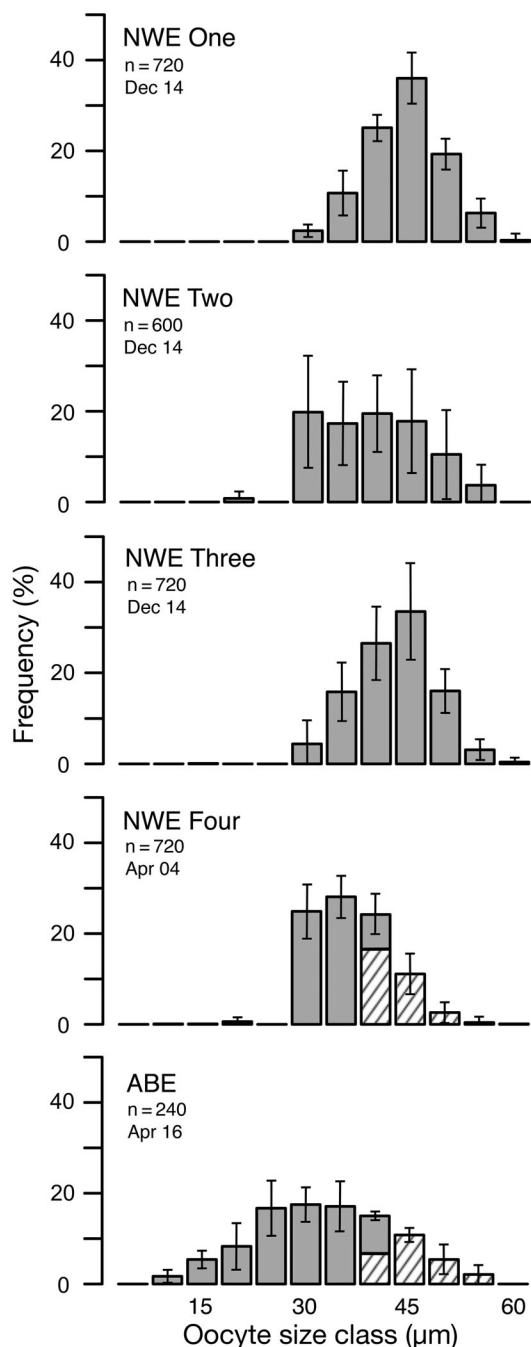
Fig. 7. Summed mussel *Bathymodiolus septemdierum* oocyte size–frequency distributions (mean ± SD) for all sampling sites: NWE One, Two, Three and Four and ABE in Lau Basin. Hatched bars: residual oocytes. Month and year of collection are noted
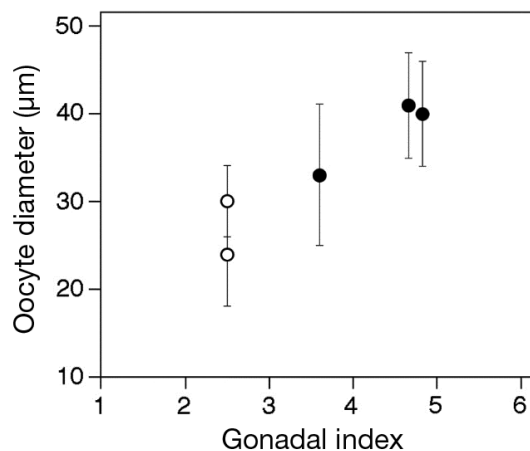

Fig. 8. Mussel *Bathymodiolus septemdierum* gonadal index corresponding to average oocyte diameter showing size increase as gametogenesis proceeds. Data do not include residual oocyte sizes. Open symbols: April collections from NWE Four and ABE; closed symbols: December collections from NWE One, Two and Three. Bars: SD

2010). As mussels are capable of moving (shifting small distances), moving to less extreme conditions can benefit stressed mussels; Nifonea imagery shows many mussels with foot extended during a move. Mottl et al. (2011) reported pH measurements in the ABE mussel bed of 7.0 (18°C), 7.2 (13°C) and 7.4 (11°C); a lower pH of 6.1 occurs only in fluids over 100°C. Within about 50 cm of our ABE sample, we saw shells with exposed calcium carbonate of dead mussels similar to pockets of shells throughout the field. Exposed calcium carbonate of shells was very rare within the NW Eifuku mussel bed (Tunnicliffe et al. 2009, this study). While a complete chemical characterization is necessary to compare the sites, we are confident that the NW Eifuku mussels experience a more persistent environment of high pCO_2 and low pH compared to those living at ABE and Nifonea.

Shell and body condition

This study confirmed that high CO_2 conditions on NW Eifuku limit *Bathymodiolus septemdierum* shell calcification in the very low saturation states for both calcite and aragonite (Tunnicliffe et al. 2009). Shells at a given volume were about half the weight of those from Nifonea and ABE. Using the pH, temperature and alkalinity values of mussel beds at ABE in Mottl et al. (2011), we calculated saturation states for both calcite and aragonite at ABE to be <0.65 (CO_2Calc programme; same constants as in Tunnicliffe et al. 2009). Yet ABE shells were highly calcified with ex-

In contrast, Nifonea has distinct biological zoning similar to that described for the ABE vents: steep gradients of hydrothermalism are reflected in animal assemblage composition in which mussels occupy patches of lesser venting (Podowski et al. 2009,

posed shell at the umbo, and some valves had repairs, probably from crab attacks. These mussels may move from damaging pH levels in the steep fluid gradients and/or expend energy to maintain deposition and execute repair. Predator-induced shell thickening is known to occur in several marine molluscs (e.g. Appleton & Palmer 1988, Palmer 1990, Robinson et al. 2014); the thickened shells of ABE mussels may be a similar response to the abundant crabs at this site.

The etched inner surfaces of NW Eifuku shells imply that, by post-deposition dissolution, the animals moderate acidosis with shell-derived HCO$_3^-$ similar to species of *Mytilus* (Lindinger et al. 1984, Michaelidis et al. 2005). Under hypercapnic conditions, pH regulation in mantle epithelial cells can be costly, and energy allocation to other fitness-sustaining processes may take precedence over shell growth and maintenance. As all NWE mussels had similar low calcification, there appears to be no incentive to maintain thicker shells in the higher pH levels. However, a minimum shell thickness is required to withstand the compressive and bending forces exerted by the muscles for shell closure. In the absence of predators, these mussels need only to maintain an intact periostracum by ensuring abrasion is minimal.

The wide range in CIs and water content reflects physiological differences among the collection sites. Compared to the reference sites, 2 of the 4 samples from NW Eifuku showed no diminished overall condition (measured with respect to shell volume). Either the mussels compensated for hypercapnia and pH, or the reference site mussels also experienced metabolic stress, or both. Condition of Nifonea mussels could be affected by the symbiotic scaleworm. Both Britayev et al. (2007) and Takahashi et al. (2012) determined that *Branchipolynoë* consume host tissue in other *Bathymodiolus* associations. No polynoids occurred in ABE mussels, yet their CIs were lower, and the dry weight to shell weight ratio was lowest of all samples. Here, a trade-off in energy allocation appears to benefit shell mass, perhaps analogous to the brittle star *Amphiura filiformis* which increases metabolic and calcification rates at the cost of muscle wasting (Wood et al. 2008). As ABE mussels were sampled close to measurements >15°C, they could be near the upper limits of their temperature (Henry et al. 2008) or sulphide (Beinart et al. 2015) tolerance. A comparison of CIs among *Bathymodiolus* species from several studies (see Table S1 in the Supplement) shows *B. septemdierum* to have among the lowest measured. In general, indices for *B. childressi*

(with methanotrophs) and *B. azoricus* (with thio- and methanotrophs) are 2 to 3 times higher.

Mussels from NW Eifuku sites One and Four had high body dry weight for a given shell weight, while in contrast, NWE Two and NWE Three mussels showed the poorest condition. The latter sample was compromised by a long delay (2 d) between collection and fixation; thus, body condition and symbiont abundance were likely diminished. The NWE Two mussels also had the highest water content, the lightest shells for volume and low dry tissue weights. Given the thin shell condition, it is likely these animals must deal with sustained stress from high pCO$_2$, diverting energy from shell maintenance to sustain body growth. Under high pCO$_2$ and limited food conditions, Melzner et al. (2011) found that fitness-sustaining processes like somatic growth and reproduction take precedence over inner shell maintenance and repair in *Mytilus edulis*. The lateral delivery of the vent fluid over the mussel bed produced low ambient temperatures that may lower metabolic demands, but also reduce saturation states of calcite and aragonite; thus calcification is relatively more difficult than at a higher temperature site.

Gill symbionts

Access to reduced compounds to support chemosynthesis influences *Bathymodiolus* condition (e.g. Smith et al. 2000). NWE One mussels had high symbiont abundance in a wide bacteriocyte layer where sample location and pH levels correspond closely to prior measures of sulphide levels well above 100 µmol l^{-1}. In comparison, NWE Two had low symbiont numbers and a narrow bacteriocyte layer. *B. septemdierum* from the Central Indian Ridge had symbiont abundances comparable to those at NWE One (1 to 13 symbionts vacuole^{-1}, bacterial layer ~20 µm; McKiness & Cavanaugh 2005) while Dubilier et al. (1998) reported a thin layer at ~2 µm in North Fiji Basin mussels, with 1 symbiont vacuole^{-1}. Several studies have discussed the flexibility of symbiont populations between vent sites with differing chemical signatures (e.g. Riou et al. 2008, Szafranski et al. 2015); Fujinoki et al. (2012) found lower symbiont abundances at sulphide levels of 0.29 compared 12.03 µmol l^{-1}. These differences suggest that symbionts are highly sensitive to changes in [H$_2$S] even across one site.

Gill ultrastructure of *B. septemdierum* is similar to other bathymodiolin mussels, although intercalary cells are less common (e.g. *B. thermophilus*; Fisher et al. 1987). In the ultraoligotrophic Marianas region, *B.*

septemdierum may rely less on suspension feeding and more on the transfer of organic carbon compounds from endosymbionts for nutrition. We also saw lysosomal degradation of bacterial endosymbionts as observed by Fiala-Médioni et al. (1986), which has been described as an additional method of obtaining energy from symbionts (Ponnudurai et al. 2017). Food supply through a large symbiont population probably supports calcification and gonad production in *B. septemdierum*, as suggested for sea urchins at high pCO$_2$ sites in the Mediterranean (Uthicke et al. 2016).

The compromised inner shell layer indicates a process similar to that in *Mytilus galloprovincialis*, which buffers haemolymph pH through shell dissolution (Michaelidis et al. 2005). As in the *Mytilus* study, NW Eifuku mussels showed diminished growth rates, as measured by daily growth bands (Tunnicliffe et al. 2009). Although growth was slower, the NWE One mussels showed a high AFDW: length ratio — similar to the reference sites — which was achieved through 'plumper' shells with less surface area (= calcium carbonate) for a given length. It is unlikely that metabolic depression was initiated as reported elsewhere (e.g. Guppy & Withers 1999, Pörtner et al. 2004, Gazeau et al. 2013) because all NW Eifuku mussels were undergoing gametogenesis and overall condition did not appear highly compromised.

Reproductive mode

B. septemdierum is functionally dioecious, but the presence of residual oocytes in functional males is evidence of protogynous hermaphroditism — the first noted for the genus. In contrast, Le Pennec & Beninger (1997) reported protandry in the same species from the North Fiji Basin, where female gametes appeared in spent male acini. Thus, sequential hermaphroditism is bi-directional in *B. septemdierum*. Male to female transition also occurs occasionally in *B. thermophilus* (Berg 1985) and *B. azoricus* (Dixon et al. 2006). Manifestation of gender can have a strong environmental component; males may dominate in poor environmental conditions because sperm production is less energetically expensive than egg generation (Russell-Hunter 1979). Lower body and gill condition in the heavily male-biased ABE mussels suggests that habitat-induced stress favours a switch to males. Maturation size in *B. septemdierum* differs between sexes, with males as small as 29 mm whereas the smallest female was 73 mm in length. Our smallest hermaphrodites were over 80 mm, indica-

ting that sex change did not happen until after female maturation size.

Gametogenesis

Bathymodiolus does not appear to divert energy from gonad maintenance under high pCO$_2$ conditions in all circumstances. With one exception, NW Eifuku mussels showed no marked evidence of compromised reproductive condition, such as premature spawning and poor physical gonadal condition. Mussels from NWE Two lagged NWE One and Three in oocyte development. As body, gill and shell condition were also lowest here, high pCO$_2$ probably lowered several aspects of fitness in this sample. Other indicators of high pCO$_2$ effects such as markedly reduced gonads (in sea urchins, Siikavuopio et al. 2007), reduced fecundity (in shrimp, Kurihara 2008) or failed spawning (in carpet clam, Range et al. 2011) were not evident.

Gametogenesis in *B. septemdierum* is similar to that described for *B. azoricus* (Dixon et al. 2006) and *B. childressi* (Tyler et al. 2007), although our staging scheme noted the presence of residual or effete gametes. Gonadal indices and oocyte size-frequency distributions provided evidence of discontinuous gametogenesis despite limited samples: mussels collected in April were in early stages of gametogenesis while December mussels were in later stages. In addition, males and females in a sample were strongly synchronized. Variation in stages among individuals from neighbouring sites may represent 'leaky' reproduction, whereby smaller spawning events occur around the central event.

Both *B. azoricus* and *B. childressi* show synchronized gametogenesis, with spawning occurring loosely around the time phytodetritus from surface production arrives at the seafloor (Dixon et al. 2006, Tyler et al. 2007). Phytodetritus may have little role in *B. septemdierum* nutrition in the northern Mariana region, where primary productivity borders on ultra-oligotrophic as measured in March 2010 (Suntsov & Domokos 2013). Le Pennec & Beninger (1997) reported discontinuous spermatogenesis in *B. septemdierum* from the North Fiji Basin in an oligotrophic region (Lemasson et al. 1990), whereas Dubilier et al. (1998) reported isotopic evidence of multiple carbon sources in mussels at North Fiji. But another signal may cue reproduction: tidal rhythms in both fluid output and in ambient currents are well-known to influence the behaviour of vent animals (e.g. Tunnicliffe et al. 1990, Cuvelier et al. 2014, Lee et al. 2015)

including *B. septemdierum*, which shows a tidal record in shell growth increments (Schöne & Giere 2005). Resuspended organics may provide the additional food source and possibly a cyclic cue in spring/neap tides. As with other vent and seep species, *B. septemdierum* reproductive patterns may reflect phylogenetic history (Tyler & Young 1999).

Trade-offs

Our expectations that the high pCO$_2$ environment on NW Eifuku would diminish mussel body condition and compromise gametogenesis were not met over all samples. The sample with the lowest pH (5.2) was also that with the most abundant gill bacteriocytes — likely because of higher sulphide access. Body condition was equal to, or greater than, reference sites in all but one sample, and reproductive tissues were healthy with gametogenesis reaching final stages. However, the stressful conditions were apparent in poorly calcified shells, low growth rates (Tunnicliffe et al. 2009) and some animals with lower body condition with respect to shell size. *B. septemdierum* appears to trade off energy allocation among shell formation, reproduction and probably acid–base moderation. The lack of brachyuran predators on NW Eifuku allows the species to maintain a minimal shell compared to other sites. Where dissolved sulphide is higher, excess energy demands imposed by high pCO$_2$/low pH conditions appear alleviated by adequate food availability through symbiont chemosynthesis: high dissolved sulphide supports dense bacterial symbionts in the gills of mussels close to fluid supply. Carbon fixation through hydrogen oxidation occurs in the thiotrophic symbionts of *B. puteoserpentis* from the Mid-Atlantic Ridge (Petersen et al. 2011); in an acidic environment, hydrogen-based metabolism may be a potential mechanism for energy acquisition in *B. septemdierum*, though this was not investigated in this study. In the larger context of ocean acidification, it is evident that good nutrition delays onset of measurable stress.

B. septemdierum has the broadest biogeographic range reported for hydrothermal vent species (Breusing et al. 2015), with a depth range from 1100 m (Monowai) to 3800 m (Mariana Trough). The species survives at temperatures from 2 to 18°C, at ΣH$_2$S to 300 µmol l^{-1} (Henry et al. 2008) and at pH values down to 5.22. It is very likely that extremes in any of these variables will reduce the fitness of individuals; but the animal can compensate in many ways, including (1) alternative nutrition sources, (2) bacte-

riocyte expansion to take advantage of dissolved sulphide availability, (3) energy diversion from or to shell maintenance, (4) sex switching in both directions to adapt to energetic costs and (5) a reproductive mode that optimizes synchronous development among neighbours but may adapt to local conditions. Other factors that support its competitive success include a long life span (Schöne & Giere 2005, Tunnicliffe et al. 2009) and mobility to follow local fluid changes. It likely has a long-range larva similar to that of *B. childressi* (Arellano et al. 2014), thus can be effective in metapopulation maintenance and invasion of new vent sites. The energy trade-offs that must occur in this species to support robust gonad development along with adaptations to a wide range of habitat conditions likely play strong roles in securing its broad biogeographic range.

LITERATURE CITED

Anderson MO, Hannington MD, Haase K, Schwarz-Schampera U, Augustin N, McConachy TF, Allen K (2016) Tectonic focusing of voluminous basaltic eruptions in magma-deficient backarc rifts. Earth Planet Sci Lett 440: 43–55

Appleton RD, Palmer AR (1988) Water-borne stimuli released by predatory crabs and damaged prey induce more predator-resistant shells in a marine gastropod. Proc Natl Acad Sci USA 85:4387–4391

Arellano SM, Van Gaest AL, Johnson SB, Vrijenhoek RC, Young CM (2014) Larvae from deep-sea methane seeps disperse in surface waters. Proc R Soc B 281:20133276

Barton A, Hales B, Waldbusser GG, Langdon C, Feely RA (2012) The Pacific oyster, *Crassostrea gigas*, shows negative correlation to naturally elevated carbon dioxide levels: implications for near-term ocean acidification effects. Limnol Oceanogr 57:698–710

Bates AE, Bird TJ, Robert K, Onthank KL, Quinn GP, Juniper SK, Lee RW (2013) Activity and positioning of eurythermal hydrothermal vent sulphide worms in a variable thermal environment. J Exp Mar Biol Ecol 448:149–155

Bednarsek N, Feely RA, Reum JCP, Peterson B, Menkel J, Alin SR, Hales B (2014) *Limacina helicina* shell dissolu-

tion as an indicator of declining habitat suitability owing to ocean acidification in the California Current Ecosystem. Proc R Soc B 281:20140123

Beinart RA, Gartman A, Sanders JG, Luther GW, Girguis PR (2015) The uptake and excretion of partially oxidized sulfur expands the repertoire of energy resources metabolized by hydrothermal vent symbioses. Proc R Soc B 282:20142811

Berg CJ (1985) Reproductive strategies of mollusks from abyssal hydrothermal vent communities. Bull Biol Soc Wash 6:185–197

Bergquist DC, Fleckenstein C, Szalai EB, Knisel J, Fisher CR (2004) Environment drives physiological variability in the cold seep mussel *Bathymodiolus childressi*. Limnol Oceanogr 49:706–715

Branch TA, DeJoseph BM, Ray LJ, Wagner CA (2013) Impacts of ocean acidification on marine seafood. Trends Ecol Evol 28:178–186

Breusing C, Johnson S, Tunnicliffe V, Vrijenhoek R (2015) Population structure and connectivity in Indo-Pacific deep-sea mussels of the *Bathymodiolus septemdierum* complex. Conserv Genet 16:1415–1430

Britayev TA, Martin D, Krylova EM, von Cosel R, Aksiuk TS (2007) Life-history traits of the symbiotic scale-worm *Branchipolynoe seepensis* and its relationships with host mussels of the genus *Bathymodiolus* from hydrothermal vents. Mar Ecol 28:36–48

Calow P (1983) Energetics of reproduction and its evolutionary implications. Biol J Linn Soc 20:153–165

Crosby M, Gale L (1990) A review and evaluation of bivalve condition index methodologies with a suggested standard method. J Shellfish Res 9:233–237

Cuvelier D, Legendre P, Laes A, Sarradin PM, Sarrazin J (2014) Rhythms and community dynamics of a hydrothermal tubeworm assemblage at Main Endeavour Field —a multidisciplinary deep-sea observatory approach. PLOS ONE 9:e96924

Dixon DR, Lowe DM, Miller PI, Villemin GR, Colaço A, Serrão-Santos R, Dixon LRJ (2006) Evidence of seasonal reproduction in the Atlantic vent mussel *Bathymodiolus azoricus*, and an apparent link with the timing of photosynthetic primary production. J Mar Biol Assoc UK 86:1363–1371

Dubilier N, Windoffer R, Giere O (1998) Ultrastructure and stable carbon isotope composition of the hydrothermal vent mussels *Bathymodiolus bevior* and *B.* sp. affinis *brevior* from the North Fiji Basin, western Pacific. Mar Ecol Prog Ser 165:187–193

Embley RW, Baker ET, Butterfield DA, Chadwick WW Jr and others (2007) Exploring the submarine ring of fire: Mariana Arc-Western Pacific. Oceanography (Wash DC) 20:68–79

Fiala-Médioni A, McKiness ZP, Dando P, Boulegue J and others (2002) Ultrastructural, biochemical, and immunological characterization of two populations of the mytilid mussel *Bathymodiolus azoricus* from the Mid-Atlantic Ridge: evidence for a dual symbiosis. Mar Biol 141:1035–1043

Fiala-Médioni A, Métivier C, Herry A, Le Pennec M (1986) Ultrastructure of the gill of the hydrothermal-vent mytilid *Bathymodiolus* sp. Mar Biol 92:65–72

Fisher CR, Childress JJ, Oremland RS, Bidigare RR (1987) The importance of methane and thiosulfate in the metabolism of the bacterial symbionts of two deep-sea mussels. Mar Biol 96:59–71

Fisher CR, Childress JJ, Arp AJ, Brooks JM and others (1988) Microhabitat variation in the hydrothermal vent mussel, *Bathymodiolus thermophilus*, at the Rose Garden vent on the Galapagos Rift. Deep-Sea Res 35:1769–1791

Flores GE, Shakya M, Meneghin J, Yang ZK and others (2012) Inter-field variability in the microbial communities of hydrothermal vent deposits from a back-arc basin. Geobiology 10:333–346

Fujinoki M, Koito T, Nemoto S, Kitada M and others (2012) Comparison of the amount of thiotrophic symbionts in the deep-sea mussel *Bathymodiolus septemdierum* under different sulfide levels using fluorescent in situ hybridization. Fish Sci 78:139–146

Gattuso JP, Magnan A, Billé R, Cheung WWL and others (2015) Contrasting futures for ocean and society from different anthropogenic CO_2 emissions scenarios. Science 349:aac4722

Gazeau F, Parker LM, Comeau S, Gattuso JP and others (2013) Impacts of ocean acidification on marine shelled molluscs. Mar Biol 160:2207–2245

Guppy M, Withers P (1999) Metabolic depression in animals: physiological perspectives and biochemical generalizations. Biol Rev Camb Philos Soc 74:1–40

Henry MS, Childress JJ, Figueroa D (2008) Metabolic rates and thermal tolerances of chemoautotrophic symbioses from Lau Basin hydrothermal vents and their implications for species distributions. Deep Sea Res I 55:679–695

Higgins E (1938) Report of the commissioner of fisheries for the fiscal year 1938. Appendix 1. Administrative report No. 300. US Bureau of Fisheries, Washington, DC

Hochachka PW, Somero GN (2002) Biochemical adaptation: mechanism and process in physiological evolution. Oxford University Press, New York, NY

IPCC (2014) Climate change 2014: synthesis report. Contribution of Working Groups I, II, and III to the Fifth Assessment Report of the Intergovernmental Panel on Climate Change. IPCC, Geneva

Kroeker KJ, Kordas RL, Crim RN, Singh GG (2010) Metaanalysis reveals negative yet variable effects of ocean acidification on marine organisms. Ecol Lett 13:1419–1434

Kurihara H (2008) Effects of CO_2-driven ocean acidification on the early developmental stages of invertebrates. Mar Ecol Prog Ser 373:275–284

Lannig G, Eilers S, Pörtner HO, Sokolova IM, Bock C (2010) Impact of ocean acidification on energy metabolism of oyster, *Crassostrea gigas* – changes in metabolic pathways and thermal response. Mar Drugs 8:2318–2339

Le Pennec M, Beninger PG (1997) Ultrastructural characteristics of spermatogenesis in three species of deep-sea hydrothermal vent mytilids. Can J Zool 75:308–316

Lee RW, Robert K, Matabos M, Bates AE, Juniper SK (2015) Temporal and spatial variation in temperature experienced by macrofauna at Main Endeavour hydrothermal vent field. Deep Sea Res I 106:154–166

Lemasson L, Charpy L, Blanchot J (1990) Biomasse et structure de tailles dans les eaux oligotrophes du Pacifique Sud-Ouest (croisière Proligo). Oceanol Acta 10:369–381

Lindinger MI, Laurén DJ, McDonald DG (1984) Acid-base balance in the sea mussel, *Mytilus edulis*. III. Effects of environmental hypercapnia on intra- and extracellular acid-base balance. Mar Biol Lett 5:371–381

Lupton J, Butterfield D, Lilley M, Evans L and others (2006) Submarine venting of liquid carbon dioxide on a Mariana Arc volcano. Geochem Geophys Geosyst 7:Q08007

McKiness ZP, Cavanaugh CM (2005) The ubiquitous mussel: *Bathymodiolus* aff. *brevior* symbiosis at the Central Indian Ridge hydrothermal vents. Mar Ecol Prog Ser 295: 183–190

Melzner F, Stange P, Trübenbach K, Thomsen J and others (2011) Food supply and seawater pCO$_2$ impact calcification and internal shell dissolution in the blue mussel *Mytilus edulis.* PLOS ONE 6:e24223

Michaelidis B, Ouzounis C, Paleras A, Pörtner HO (2005) Effects of long-term moderate hypercapnia on acid–base balance and growth rate in marine mussels *Mytilus galloprovincialis.* Mar Ecol Prog Ser 293:109–118

Mills EL, Pittman K, Munroe B (1982) Effect of preservation on the weight of marine benthic invertebrates. Can J Fish Aquat Sci 39:221–224

Mottl MJ, Seewald JS, Geoffrey Wheat C, Tivey MK and others (2011) Chemistry of hot springs along the Eastern Lau Spreading Center. Geochim Cosmochim Acta 75: 1013–1038

Nix ER, Fisher CR, Vodenichar J, Scott KM (1995) Physiological ecology of a mussel with methanotrophic endosymbionts at three hydrocarbon seep sites in the Gulf of Mexico. Mar Biol 122:605–617

Page HM, Fiala-Médioni A, Fisher CR, Childress JJ (1991) Experimental evidence for filter-feeding by the hydrothermal vent mussel, *Bathymodiolus thermophilus.* Deep-Sea Res A Oceanogr Res Pap 38:1455–1461

Palmer AR (1990) Effect of crab effluent and scent of damaged conspecifics on feeding, growth, and shell morphology of the Atlantic dogwhelk *Nucella lapillus* (L.). Hydrobiologia 193:155–182

Pan TCF, Applebaum SL, Manahan DT (2015) Experimental ocean acidification alters the allocation of metabolic energy. Proc Natl Acad Sci USA 112:4696–4701

Petersen JM, Zielinski FU, Pape T, Seifert R and others (2011) Hydrogen is an energy source for hydrothermal vent symbioses. Nature 476:176–180

Podowski EL, Moore TS, Zelnio KA, Luther GW, Fisher CR (2009) Distribution of diffuse flow megafauna in two sites on the Eastern Lau Spreading Center, Tonga. Deep Sea Res I 56:2041–2056

Podowski EL, Ma S, Luther GW III, Wardrop D, Fisher CR (2010) Biotic and abiotic factors affecting distributions of megafauna in diffuse flow on andesite and basalt along the Eastern Lau Spreading Center, Tonga. Mar Ecol Prog Ser 418:25–45

Ponnudurai R, Kleiner M, Sayaverda L, Petersen JM and others (2017) Metabolic and physiological interdependencies in the *Bathymodiolus azoricus* symbiosis. ISME J 11:463–477

Pörtner HO (2008) Ecosystem effects of ocean acidification in times of ocean warming: a physiologist's view. Mar Ecol Prog Ser 373:203–217

Pörtner HO, Langenbuch M, Reipschlager A (2004) Biological impact of elevated ocean CO$_2$ concentrations: lessons from animal physiology and earth history. J Oceanogr 60: 705–718

Range P, Chícharo MA, Ben-Hamadou R, Piló D and others (2011) Calcification, growth and mortality of juvenile clams *Ruditapes decussatus* under increased pCO$_2$ and reduced pH: variable responses to ocean acidification at local scales? J Exp Mar Biol Ecol 396:177–184

Ries JB, Cohen AL, McCorkle DC (2009) Marine calcifiers exhibit mixed responses to CO$_2$-induced ocean acidification. Geology 37:1131–1134

Riou V, Halary S, Duperron S, Bouillon S and others (2008) Influence of CH$_4$ and H$_2$S availability on symbiont distribution, carbon assimilation and transfer in the dual symbiotic vent mussel *Bathymodiolus azoricus.* Biogeosciences 5:1681–1691

Robinson EM, Lunt J, Marshall CD, Smee DL (2014) Eastern oysters *Crassostrea virginica* deter crab predators by altering their morphology in response to crab cues. Aquat Biol 20:111–118

Rossi G (2016) The reproductive and physiological condition of a deep-sea mussel (*Bathymodiolus septemdierum* Hashimoto & Okutani, 1994) living in extremely acidic conditions. MSc thesis, University of Victoria

Russell-Hunter WD (1979) A life of invertebrates. MacMillan Publishing, New York, NY

Schöne BR, Giere O (2005) Growth increments and stable isotope variation in shells of the deep-sea hydrothermal vent bivalve mollusk *Bathymodiolus brevior* from the North Fiji Basin, Pacific Ocean. Deep Sea Res I 52: 1896–1910

Seed R (1969) The ecology of *Mytilus edulis* L. (Lamellibranchiata) on exposed rocky shores. Oecologia 3: 277–316

Seibel BA, Walsh PW (2003) Biological impacts of deep-sea carbon dioxide injection inferred from indices of physiological performance. J Exp Biol 206:641–650

Siikavuopio SI, Mortensen A, Dale T, Foss A (2007) Effects of carbon dioxide exposure on feed intake and gonad growth in green sea urchin, *Strongylocentrotus droebachiensis.* Aquaculture 266:97–101

Silverman J, Schneider K, Kline DI, Rivlin T, Rivlin A, Hamylton S (2014) Community calcification in Lizard Island, Great Barrier Reef : a 33 year perspective. Geochim Cosmochim Acta 144:72–81

Smith EB, Scott KM, Nix ER, Korte C, Fisher CR (2000) Growth and condition of seep mussels (*Bathymodiolus childressi*) at a Gulf of Mexico brine pool. Ecology 81: 2392–2403

Sokolova IM, Frederich M, Bagwe R, Lannig G, Sukhotin AA (2012) Energy homeostasis as an integrative tool for assessing limits of environmental stress tolerance in aquatic invertebrates. Mar Environ Res 79:1–15

Suntsov A, Domokos R (2013) Vertically migrating micronekton and macrozooplankton communities around Guam and the Northern Mariana Islands. Deep Sea Res I 71:113–129

Szafranski KM, Piquet B, Shillito B, Lallier FH, Duperron S (2015) Relative abundances of methane- and sulfuroxidizing symbionts in gills of the deep-sea hydrothermal vent mussel *Bathymodiolus azoricus* under pressure. Deep Sea Res I 101:7–13

Takahashi Y, Sasaki Y, Chikaraishi Y, Tsuchiya M and others (2012) Does the symbiotic scale-worm feed on the host mussel in deep-sea vent fields? Res Org Geochem 28:23–26

Tunnicliffe V, Garrett JF, Johnson HP (1990) Physical and biological factors affecting the behaviour and mortality of hydrothermal vent tubeworms (vestimentiferans). Deep-Sea Res A Oceanogr Res Pap 37:103–125

Tunnicliffe V, Davies KTA, Butterfield DA, Embley RW, Rose JM, Chadwick WW Jr (2009) Survival of mussels in extremely acidic waters on a submarine volcano. Nat Geosci 2:344–348

Turnipseed M, Knick KE, Lipcius RN, Dreyer J, Van Dover CL (2003) Diversity in mussel beds at deep-sea hydro-

thermal vents and cold seeps. Ecol Lett 6:518–523

Tyler PA, Young CM (1999) Reproduction and dispersal at vents and cold seeps. J Mar Biol Assoc UK 79:193–208

Tyler PA, Young CM, Dolan E, Arellano SM, Brooke SD, Baker M (2007) Gametogenic periodicity in the chemosynthetic cold-seep mussel 'Bathymodiolus' childressi. Mar Biol 150:829–840

Uthicke S, Ebert T, Liddy M, Johansson C (2016) *Echinometra* sea urchins acclimatized to elevated pCO_2 at volcanic vents outperform those under present-day pCO_2 conditions. Glob Change Biol 22:2451–2461

Wicks LC, Roberts JM (2012) Benthic invertebrates in a high-CO_2 world. Oceanogr Mar Biol Annu Rev 50:127–188

Wood HL, Spicer JI, Widdicombe S (2008) Ocean acidification may increase calcification rates, but at a cost. Proc R Soc B 275:1767–1773